Zebrafish as research model to study Gaucher disease: Insights into molecular mechanisms

Lelieveld, L.T.

CHAPTER 8

α-Galactosidases in zebrafish

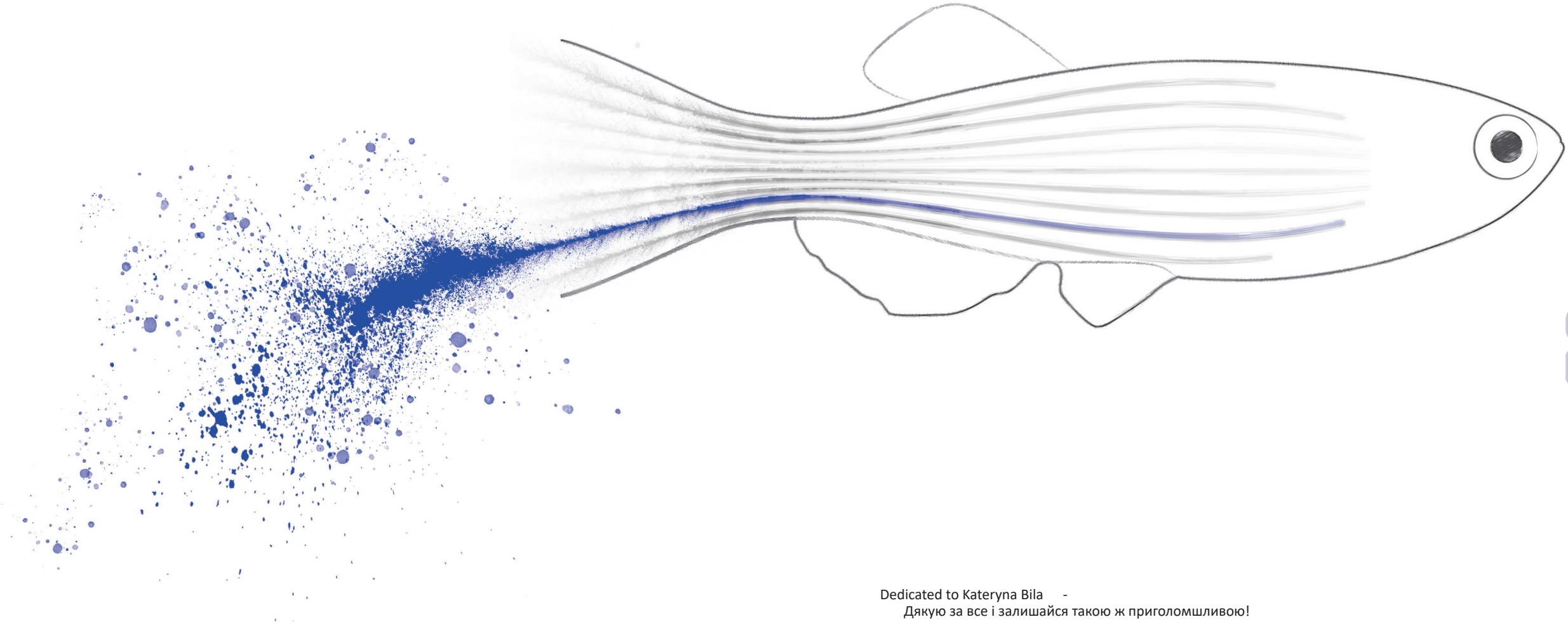

Dedicated to Kateryna Bila -
Дякую за все і залишайся такою ж приголомшливою!

Abstract

Human α-galactosidase A (α-GAL A) is responsible for the hydrolysis of terminal α-galactosyl moieties from glycosphingolipids in lysosomes. Mutations in the X-linked *GLA* gene resulting in deficient α-GAL A cause the lysosomal storage disorder Fabry disease. The highly homologous enzyme, α-N-acetylgalactosaminidase (α-NAGAL), primarily cleaves terminal N-acetylgalactosamine moieties from glycocojugates, but it is *in vitro* also active towards α-galactosides. This chapter investigates the presence of α-galactosidase enzymes in zebrafish embryonic fibroblast cells, zebrafish larvae (5 days post-fertilization) and organs of adult fish. The zebrafish genome annotates one α-Gal A and one α-Nagal orthologue. The presence of α-Gal A and α-Nagal proteins in zebrafish cells and larvae was confirmed by chemical proteomics using an α-Gal configured activity-based probe (ABP). Both enzymes have N-linked glycans and a comparable molecular weight of 45 kDa as determined by SDS-PAGE. Fluorogenic α-galactoside and α-N-acetylgalactosaminide substrates reveal considerable α-Nagal activity in zebrafish larvae and adult organs. α-Gal A activity is lower than α-Nagal activity, but higher in fertilized eggs, reproductive organs, liver and kidney. Interestingly, no Gb3 could be detected using sensitive LC-MS/MS methods in any of the studied zebrafish materials such as cells, larvae, brain, liver, kidney and testis. The absence of the lipid Gb3 is consistent with the absence of a gene encoding lactosylceramide 4-α-galactosyltransferase (A4gGALTt; Gb3 synthase) in zebrafish or any other teleost species. HEK293T cells lacking endogenous α-GAL A were generated using CRISPR/Cas9 technology. The increase in endogenous Gb3 levels in these cells could be comparably corrected by over-expression of either human α-GAL A or zebrafish α-Gal A. These findings indicate that zebrafish α-Gal A can hydrolyse the endogenous substrate Gb3 in the cellular setting, however it seems that it is not able to hydrolyse the artificial substrate NBD-Gb3 *in vitro*. The role of the conserved α-galactosidase encoded by the *gla* gene in the zebrafish remains elusive. It is envisioned that *gla*$^{-/-}$ zebrafish expressing human A4GALT might render a useful Fabry disease model. The comparison of such fish with those with a concomitant *asha1b* KO might assist the investigation of the specific impact of excessive lysoGb3 in Fabry disease pathology.

Introduction

Human α-galactosidase A (α-Gal A; E.C.3.2.1.22, Uniprot accession P06280) is encoded by the *GLA* gene at locus Xq22 and responsible for the hydrolysis of terminal α-linked galactosyl moieties of primarily the α-1,4-linked glycosphingolipids globotriaosylceramide (Gb3) and galabiaosylceramide (diGalCer) in lysosomes[1,2]. In addition, ABO blood group antigens are determined by terminal α-1,3-Gal and/or α-1,3-linked N-acetylgalactosamine (GalNAc) of glycolipids and glycoconjugates and antibodies against the opposite blood group antigens are of clinical importance in transfusion and transplantation[3].

Deficiency of α-Gal A leads to Fabry disease, an X-linked lysosomal storage disorder which is characterized by lysosomal accumulation of the globoside Gb3, the deacylated globotriaosylsphingosine (lysoGb3), diGalCer and blood group B GSLs in tissues as well as increased levels in body fluids[4-6]. Heart and kidney tissues are often affected in Fabry male patients who may develop clinical symptoms such as angiokeratoma, anhidrosis, acroparesthesias, gastrointestinal complaints, cardiomyopathy, cerebrovascular disease, renal insufficiency and spontaneous or triggered pain episodes[2].

In the last decade, several cyclophellitol-configured activity-based probes (ABPs) have been developed as chemical tools to study corresponding retaining glycosidase enzymes and assist the diagnosis of lysosomal storage disorders stemming from enzyme deficiencies including, but not limited to, Gaucher disease, Fabry disease and Krabbe disease[7-9]. These ABPs bind in a mechanism-based irreversible manner to the catalytic nucleophile of the retaining glycosidase, while the attached fluorophore or biotin allows detection of the target enzymes[10]. The fluorescent α-Gal configured cyclophellitol aziridine ABP has been shown to label α-Gal A in human, mouse and plant material[8,11]. The α-Gal configured ABP also labels the homologous N-acetyl-galactosaminidase (α-NAGAL), which has arisen by a gene duplication[11,12]. The α-NAGAL enzyme specifically hydrolyses terminal α-galactose moieties with a N-acetyl substituent on the 2-position of the galactose sugar (α-GalNAc) and mutations in the *NAGA* gene lead to the very rare Schindler disease[13,14]. However due to structural differences, α-NAGAL can also accommodate and hydrolyse α-galactose configured lipids *in vitro*, while α-GAL A can only hydrolyse α-galactose moieties[15,16]. Modified α-NAGAL enzymes have been developed as possible enzyme replacement therapy for Fabry disease enabling Gb3 and lyso-Gb3 corrections without the immunological cross-reactivity that can occur with recombinant α-Gal A treatment[16-18].

The aim of the present study was to characterize α-galactosidase enzymes in zebrafish materials including embryonic cells, larvae of 5 days post-fertilization (5 dpf) and organs of adult fish. The presence of both α-Gal A and α-Nagal was confirmed using a combination of mRNA analysis, activities towards artificial α-Gal substrates as well as labelling and identification of the corresponding glycosidases using α-Gal configured ABPs. The physiological role of α-Gal A in the zebrafish remains elusive since no Gb3 has been found in any of the tested zebrafish materials.

Results

Presence of α-galactosidase enzymes in zebrafish cells and larvae

Firstly, artificial fluorogenic substrates 4-methylumbelliferyl α-D-galactopyranoside (4MU-α-Gal) and 4-MU α-D-N-acetylgalactosaminide (4MU-α-GalNAc) were used to study the occurrence of corresponding hydrolytic activities in homogenates of cultured zebrafish embryonic fibroblasts (ZF4 cells) and a pool of 5 dpf zebrafish larvae. Activity towards both substrates was observed with an optimum around pH 4.0-4.5 (**Figure 1**). The activity towards 4MU-α-Gal in lysates of zebrafish cells was much higher than activity towards 4MU-α-GalNAc (**Figure 1A**; black and grey circles for 4MU-α-Gal and 4MU-α-GalNAc respectively). Only a small amount of activity towards 4MU-α-Gal was lost upon inhibition of the suspected α-Nagal enzyme with a high concentration of the α-GalNAc (NAGA) sugar (**Figure 1A**; open circles, incubation with 200 mM final concentration of α-GalNAc).

In lysates of zebrafish larvae, the activity towards 4MU-α-GalNAc was higher than that towards 4MU-α-Gal (**Figure 1B**; black and grey circles for 4MU-α-Gal and 4MU-α-GalNAc respectively). About 50% of hydrolysis of 4MU-α-Gal could be inhibited by the presence of 200 mM α-GalNAc (**Figure 1A**; open circles, incubation with α-GalNAc). An apparent IC50 of 11 mM was noted for α-GalNAc regarding 4MU-α-GalNAc activity (**Supplementary Figure 1**). In the presence of 200 mM of α-GalNAc the residual α-Nagal activity was only 5%. Thus, activity towards 4MU-α-Gal can be differentiated in two components: activity inhibitable by α-GalNAc (zebrafish α-Nagal), and activity that is not inhibitable with the sugar,(zebrafish α-Gal A), analogous to the situation in mammalian cells in tissues.

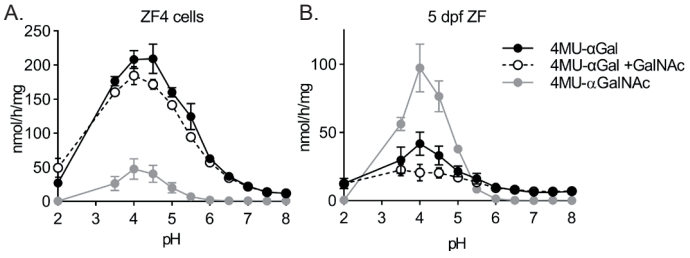

Figure 1 | Hydrolytic activity of zebrafish cells and larvae towards 4MU-α-Gal and 4MU-α-GalNAc
Activity towards 4MU-α-Gal (black) and 4MU-α-GalNAc (grey) at a range of pH values (pH 2-8) in homogenates of zebrafish embryonic cells **(A)** and zebrafish larvae of 5 dpf **(B)**. Specific activity of α-Gal A was measured by blocking α-Nagal activity using 200 mM GalNAc sugar (black, open circles). Activity is measured from three independent homogenate preparations. Data is depicted as mean ± SD.

Next, the effect of different α-galactose configured cyclophellitol aziridines was tested in cell and larvae lysates by measuring residual enzymatic activity towards 4MU-α-Gal and 4MU-α-GalNAc. Tested were ME737 and ME539 extended with an alkyl moiety at the nitrogen and TB474 conjugated further with a Cy5 fluorophore (see **Supplementary Figure 2** for structures of the inhibitors). The three compounds inhibited both α-Gal A and α-Nagal activities, with low micromolar apparent IC_{50} values (**Figure 2A** and **B**, **Table 1**). The Cy5 configured ABP (TB474) was more potent in inactivating α-galactosidase activity in the ZF4 cell and zebrafish larvae lysates than the compounds without the bulky fluorescent group (ME737 and ME737).

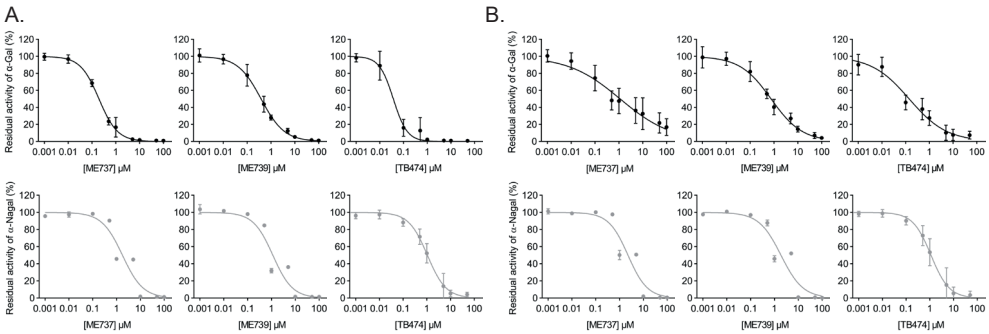

Figure 2 | Potency of α-Gal configured cyclophellitol aziridine inhibitors for α-Gal and α-Nagal
Residual activity towards 4MU-α-Gal (black) and 4MU-α-GalNAc (grey) for α-Gal A and α-Nagal respectively, in cell homogenates of ZF4 cells **(A)** and 5 dpf zebrafish larvae **(B)** treated *in vitro* with the α-Gal configured inhibitors ME737, ME739 and ABP TB474. Residual activity is measured from three independent incubations using different homogenates. Data is depicted as mean ± SD.

Table 1 | Apparent IC_{50} values of α-Gal configured ME737, ME739 and ABP TB474 for *in vitro* inhibition of α-Gal A and α-Nagal enzymes in homogenates of ZF4 cells and 5 dpf zebrafish larvae (ZF).

	α-Gal A		α-Nagal	
Compound	**ZF4 cells**	**ZF (5 dpf)**	**ZF4 cells**	**ZF (5 dpf)**
ME737 (μM)	0.197 ± 0.044	1.129 ± 1.152	1.770 ± 1.107	2.264 ± 1.56
ME739 (μM)	0.385 ± 0.113	0.755 ± 0.321	v1.144 ± 0.742	1.878 ± 1.353
TB474 (ABP) (μM)	0.037 ± 0.019	0.141 ± 0.098	1.058 ± 0.334	1.123 ± 0.436

In order to visualize the α-Gal enzymes, homogenates were incubated with the α-Gal configured ABP (TB474) for 30 min, proteins were separated using SDS-PAGE and labelled proteins were detected by in-gel fluorescence scanning. An ABP-enzyme complex with an apparent molecular weight of 45 kDa was detected in both cell and larvae lysate (**Figure 3A**; +ABP (TB474)). The intensity of this enzyme-ABP complex was significantly less, when the homogenates were pre-incubated with non-fluorescent α-Gal configured cyclophellitol aziridine inhibitor ME739 (**Figure 3A**). The intensity of the other labelled bands was not competed with ME739, indicating aspecific labelling of abundant proteins in the zebrafish material.

After translation, α-Gal enzymes are modified with high-mannose N-linked glycans acquiring terminal mannose 6-phosphate moieties that mediate transport of correctly folded enzyme to lysosomes[19]. Removal of all N-linked glycans with PNGase F digestion led to a reduction of the molecular weight of ABP-labelled enzyme from to 40 kDa, both for enzyme in homogenates of ZF4 cells and zebrafish larvae (**Figure 3B**). Fabrazyme, the recombinant human α-GAL A used to treat Fabry patients, also showed a quite comparable reduction of molecular weight following PNGase F digestion. Next, the binding to concanavalin A (ConA)-Sepharose beads was examined for the zebrafish proteins that are labelled with ABP. The lectin beads bind to the N-linked glycans in glycoproteins without interference of the active site and therefore allow subsequent activity assays. The ± 45 kDa protein labelled with ABP bound to the ConA beads, both for homogenates of ZF4 cells and 5 dpf larvae (**Figure 3C**). Hydrolysis of 4-MU-α-Gal A and 4MU-α-NAGA was nearly absent in the unbound fraction, indicating binding of the majority of active enzymes to the lectin beads (**Supplementary Figure 3**).

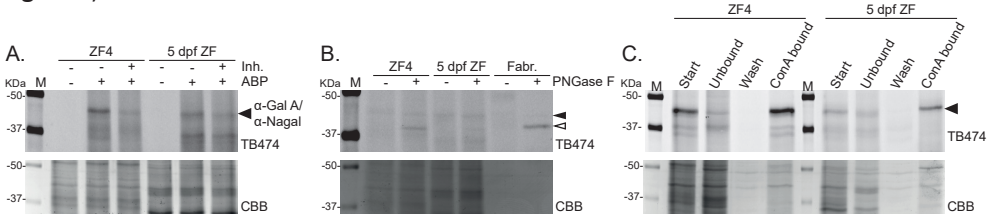

Figure 3 | *In vitro* labelling of α-Gal A and α-Nagal with α-Gal configured ABP
(A) Labelling of homogenates of ZF4 cells and a pool of 5 dpf zebrafish larvae with α-Gal configured ABP (TB474, 1μM) in the absence or presence of inhibitor ME739 (50 μM). **(B)** Homogenates and recombinant α-Gal A (Fabrazyme) were labelled with ABP TB474, before deglycosylation using PNGase F. Apparent deglycosylated protein was depicted with the open triangle. **(C)** Glycoproteins were enriched using Concanavalin A (ConA)-Sepharose beads. Start material, supernatant (unbound), wash and ConA bound material were collected and α-Gal A and α-Nagal was visualized using ABP TB474 in equal volumes relative to the starting material. Coomassie Brilliant Blue (CBB) was used as protein loading control in A-C.

Prediction of α-galactosidase and N-acetylgalactosaminidase in zebrafish genome

The zebrafish genome was evaluated for orthologues of human α-galactosidase A (Uniprot code P06280) using a protein blast. Two zebrafish orthologues were found (F1Q5G5 and F1QR55). Only F1Q5G5 showed a corresponding *gla* gene (ncbi code NM_001006103), located on chromosome 14. The genomic location of F1QR55 is allocated to chromosome 14 as well, however annotated as alternative chromosome. The two predicted proteins have 95% identity, whereby F1QR55 misses part of the N-terminal sequence of F1Q5G5. The *in silico* data suggest that only one annotated α-Gal A is expressed, while the other likely arises from genetic variation among fish. The zebrafish α-Gal A F1Q5G5 precursor protein shows 67% identity with its human α-Gal A counterpart. The predicted mature zebrafish α-Gal A contains 389 amino acids, slightly less compared to the 398 polypeptide of human α-Gal A. The zebrafish genome also shows one orthologue of human α-N-acetylgalactosaminidase (Uniprot code P17050). The zebrafish *naga* gene is located on chromosome 4 and two encoding transcripts are annotated, A0A2R8QPJ2 of 415 residues and A0A0R4IJL2 of 437 residues. Only the longer α-Nagal enzyme has a predicted signal peptide (A0A0R4IJL2). The predicted mature zebrafish α-Nagal polypeptide has 420 amino acids, compared to 394 amino acids of the human α-NAGAL.

Identification of α-galactosidase enzymes in zebrafish

ABP ME741, containing a biotin tag (see **Supplementary Figure 1**), was used to isolate ABP-reactive proteins from both the zebrafish cell and larvae homogenate and to subsequently establish their identity by proteomics with a similar streptavidin pull down based procedure as used earlier[11]. Peak lists were searched against the UniProt database of *Danio rerio*. In this manner, among the ABP-reactive proteins in the zebrafish cell homogenate the two zebrafish α-Gal A enzymes and two annotated enzymes of α-Nagal were detected. Both α-Gal A and α-Nagal were detected in two of the three independent experiments (**Table 2**). Among the ABP-reactive proteins in the homogenate of pools of 5 dpf zebrafish larvae, only the two annotated α-Gal A enzymes were detected, even though activity towards 4MU-α-Nagal was measured in this material. Likely, the enzymes are not abundant enough to be always detected with the used chemical proteomics method.

The detected peptide sequences (**Supplementary Table 1**) were compared to the predicted amino acid sequences of α-Gal A an α-Nagal (underlined in **Supplementary Figure 4**). All detected peptide sequences were judged to be specific for one of the two enzymes. In conclusion, the ABP-based chemical proteomics method confirmed the presence of both α-Gal A and α-Nagal proteins in the zebrafish materials investigated.

Table 2 | Overview of chemical proteomics experiments using α-Gal ABP (ME741) in homogenate of ZF4 cell (performed 3 independent times) and 5 dpf zebrafish larvae (performed 2 independent times).
ND = not detected, - = experiment not performed

				Experiment 1 (25-10-2018)			Experiment 2 (09-11-2018)			Experiment 3 (10-01-2019)		
		Found	Mass (kDa)	Score	Matched peptides	Coverage (%)	Score	Matched peptides	Coverage (%)	Score	Matched peptides	Coverage (%)
ZF4 cells	**α-Gal A:** F1Q5G5	2/3	46.8	6555	13	31	1787	14	37	ND		
	α-Gal A: F1QR55	2/3	37.5	6090	10	31	1704	10	34	ND		
	α-Nagal: A0A0R4IJL2	2/3	49.8	218.4	4	8.5	ND			1311	6	14
	α-Nagal; A0A2R8QPJ2	2/3	47.4	218.4	4	8.9	ND			1311	6	15
5 dpf ZF	**A-Gal A:** F1Q5G5	2/2	46.8		-		145	5	12.5	289	9	25
	A-Gal A: F1QR55	2/2	37.5				141	4	15.5	280	8	28
	α-Nagal: A0A0R4IJL2	0/2					ND			ND		
	α-Nagal; A0A2R8QPJ2	0/2					ND			ND		

Alignment and evaluation of zebrafish α-Gal A compared to human

The structure of human α-Gal A has been solved by X-ray crystallography and revealed that α-Gal A is a homodimeric glycoprotein[15]. Alignment of human α-Gal A with zebrafish α-Gal A (isoform F1Q5G5) indicates conservation of large stretches of amino acids. Moreover, several important features and residues are conserved in the zebrafish α-Gal A protein sequence. The cysteine residues forming five disulfide bonds are conserved, however only one N-linked glycan site is conserved in the zebrafish α-Gal A (**Figure 4**, orange for cysteine residues and green for N-glycosylation sites respectively). Importantly, the catalytic nucleophile and acid/base residues are conserved in zebrafish α-Gal A (**Figure 4**, red; human catalytic nucleophile D170 and acid/base D231) as well as residues with side chains thought to have primary interactions with the α-galactose moiety[15] (**Figure 4**; W47, D92, D93, Y134, K168, E203, L206, Y207, R227 and M267 in blue and C142 and C172 in orange).

```
                    |          |          |          |          |          |
Human               MQLRNPELHLGCALALRFLALVSWDIPGARALDNGLARTPTMGWLHWERFMCNLDCQEEP 60
Zebrafish           -----------MRASIIVVIGLVCLLVPAAALDNGLALTPTMGWLHWERFMCNTDCDADP
                                           * ******* *************** **: :*
                    |          |          |          |          |          |
Human               DSCISEKLFMEMAELMVSEGWKDAGYEYLCIDDCWMAPQRDSEGRLQADPQRFPHGIRQL 120
Zebrafish           QNCIREELFMQMADVMVKEGWKDAGYEFVCIDDCWPSQQRDAQGRLQADPKRFPSGIKKL
                    :.** *:***:**::**.*********::****** : ***::*******:*** **::*
                    |          |          |          |          |          |
Human               ANYVHSKGLKLGIYADVGNKTCAGFPGSFGYYDIDAQTFADWGVDLLKFDGCYCDSLENL 180
Zebrafish           ADYVHSKGLKLGIYADVGTKTCAGYPGSLGYYDIDAKTFADWGVDLLKFDGCFMPDWHQL
                    *:****************.*****:***:*******:***************:  . .:*
                    |          |  #  #    |          |          |          |
Human               ADGYKHMSLALNRTGRSIVYSCEWPLYMWPFQKPNYTEIRQYCNHWRNFADIDDSWKSIK 240
Zebrafish           GEGYINMSSALNQTGRSIVYSCEWPLYEWQHQQPDYEAIRKTCNHWRNYGDVYDQWTSVK
                    .:** :** ***:*************** * .*:*:*  **: ******:.*: *.*.*:*
                    |          |          |          |          |          |
Human               SILDWTSFNQERIVDVAGPGGWNDPDMLVIGNFGLSWNQQVTQMALWAIMAAPLFMSNDL 300
Zebrafish           SILDWTAEKQKIVVPVAGPGGWNDPDMLIIGNFGLSRDQQQTQMALWAIMAAPLLMSNDL
                    ******: :*: :* *************:******* :** *************:*****
                    |          |          |          |          |          |
Human               RHISPQAKALLQDKDVIAINQDPLGKQGYQLRQGDNFEVWERPLSGLAWAVAMINRQEIG 360
Zebrafish           RDICPKAKELLQNKQIIAINQDPLGKQGYRILKADSFELWERPLSGNRLAVAVMNRQEIG
                    *.*.*:** ***:*::**************:: :.*.**:*******   ***::******
                    |          |          |          |          |          |
Human               GPRSYTIAVASLGKGVACNPACFITQLLPVKRKLGFYEWTSRLRSHINPTGTVLLQLENT 420
Zebrafish           GPRRFTISVAIMPSWKLCNPKCNVTQIMPTYKEMGVQNLLSEVVVQVNPTGTTLLTVNPL
                    *** :**:** : .   *** * :**::*. :::*. :  *.:  ::*****.** ::
Human               MQMSLKDLL
Zebrafish           ---------
```

Figure 4 | Alignment of human a-GAL A with zebrafish α-Gal A.
The amino acid sequences of the pro-protein of human α-GAL A (Uniprot P06280) and zebrafish α-Gal A (Uniprot F1Q5G5) were aligned using Clustal Omega[20]. ***** indicates a conserved residue, : a strongly similar residue and . a weakly similar residue. The signal peptide is predicted using SingalP-5.0[21] and depicted in purple. The catalytic Asp residues are depicted in red, Asn residues with reported N-linked in green, the cysteine residues forming five disulfide bridges in orange and residues interacting and stabilizing the α-galactose in blue. The Glu and Leu residues which form specificity of the α-galactose moiety are emphasized with #.

The protein sequence and structure of α-GAL A and α-NAGAL enzymes are quite similar[15]. The substrate specificity for either a hydroxyl or a N-acetyl substituent on the 2-position of the α-galactose moiety is thought to arise from the side chains of two amino acids in the β5-α5 loop. The side chains of E203 and L206 of human α-GAL A sterically block the larger N-acetyl substituent. The residues of α-NAGAL at the two positions are serine and alanine and these side chains do not block the N-acetyl group and tolerate a

hydroxyl group. Alignment of zebrafish α-Gal with α-Nagal (isoform A0A0R4IJL2) indicates conservation of the residues involved in the reported interactions with the α-galactose or N-acetylgalactosamine moiety (depicted in blue in **Supplementary Figure 4**). Moreover, the Glu and Leu residues are present in zebrafish α-Gal A, while Ser and Ala residues are present in zebrafish α-Nagal (**Figure 4**; # for human and zebrafish α-Gal A and **Supplementary Figure 4**; # for zebrafish α-Gal A and α-Nagal).

In vivo inhibition of α-Gal A does not show lipid abnormalities

Next, it was attempted to examine the physiological role of the zebrafish α-galactosidase enzymes *in vivo*. First it was established which concentration of the α-Gal inhibitors ME737 and ME739 led to complete inhibition of α-galactosidase activities in cultured cells and developing zebrafish larvae. A concentration of 1 µM ME737 and 24 hours of incubation was enough to block most of the α-Gal activity in cultured ZF4 cells, which showed residual α-Nagal activity (**Figure 5A**). Incubation of developing zebrafish larvae from fertilization up to 5 dpf with 100 µm ME737 or ME739 led to a reduction in α-Gal and α-Nagal activity (**Figure 5B**). High concentrations of ME737 and ME739 were used to study the glycosphingolipid changes in developing zebrafish larvae by earlier established LC-MS/MS methods[22]. No significant change was found in neutral glycosphingolipids such as lactosylceramide, glucosylceramide or ceramide (**Figure 5C**). No Gb3 was detected in samples of zebrafish larvae, neither in those of α-Gal inhibitor treated fish (**Supplementary Figure 5A**).

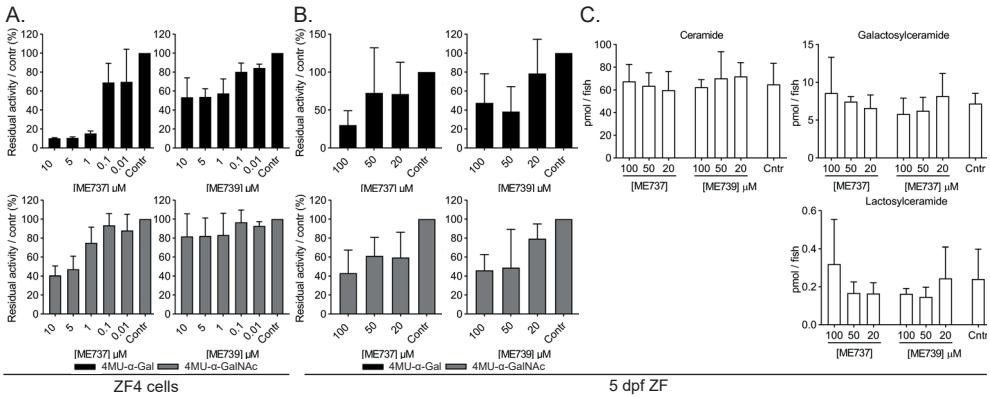

Figure 5 | *in vivo* inhibition of α-Gal A and α-Nagal

(A) ZF4 cells were treated with different concentrations ME737 or ME739 (0.1-10 µM) for 24 hours and residual activity towards 4MU-α-Gal (black bars) and 4MU-α-GalNAc (grey bars) was measured. Data is obtained from three individual incubations and depicted as mean ± SD. **(B)** Developing zebrafish embryos were treated with ME737 or ME739 (20-100 µM) for 5 days. Residual activity towards 4MU-α-Gal (black bars) and 4MU-α-GalNac (grey bars) was measured in homogenates of a pool of 3 zebrafish. Data is obtained from three individual incubations and depicted as mean ± SD. **(C)** Ceramide, galactosylceramide and lactosylceramide levels were measured of individual zebrafish larvae (5 dpf) treated with 100, 50 or 20 µM (n = 4) and DMSO treated controls (n = 7) in pmol/fish. Data is obtained from two independent incubations and depicted as mean ± SD.

Gla expression and α-Gal A activity in adult organs, but no Gb3

Next, experiments were performed to analyse the specific mRNA expression, α-galactosidase activity and the glycosphingolipid composition of developing zebrafish embryos (t = 0 – 5 dpf) as well as different organs. Evaluation of specific mRNA expression using RT-qPCR showed highest *gla* expression in fertilized eggs, brain and testis, while expression of *naga* appeared highest in fertilized eggs, brain, fin and spleen (**Figure 6A**). The expression of *naga* mRNA was relatively higher than *gla* mRNA, likely corresponding to the relatively higher activity towards 4MU-α-GalNAc in the measured materials (**Figure 6A** and **6C**). High specific α-Gal A activity was found in the liver, kidney, reproductive organs and fertilized zebrafish eggs (0 dpf) (**Figure 6B** and **Supplementary Figure 6**). Interestingly, the lipid Gb3 was not detected in brain, liver, kidney, testis or ovary tissues either (**Supplementary Figure 5A**).

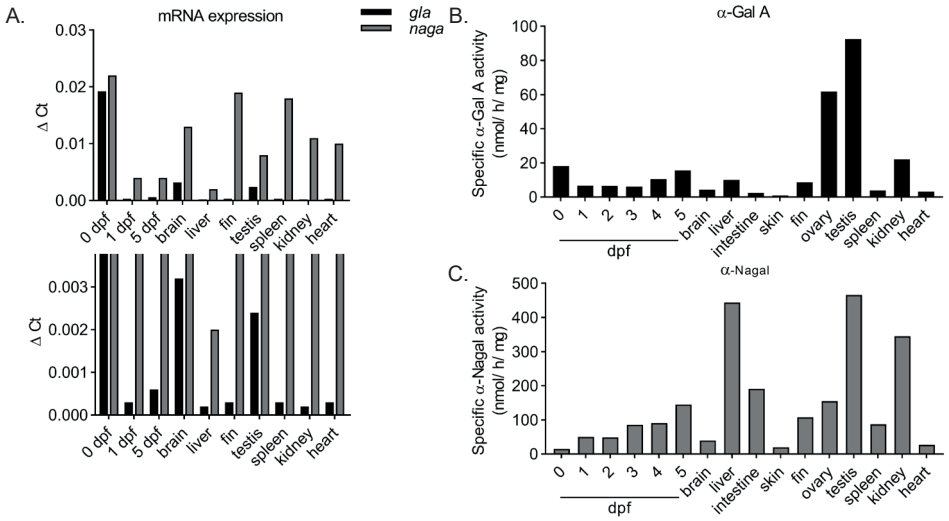

Figure 6 | mRNA expression and activity in developing zebrafish and adult organs
(A) mRNA levels of *gla* and *naga* in developing zebrafish embryos (0, 1 and 5 dpf) and adult fish organs and tissue (brain, liver, fin, testis, spleen, kidney and heart) analysed using RT-qPCR. Data is normalized using *Ef1α* and *rpl13α*, in technical duplicate and depicted as relative expression compared to the housekeeping genes. An inset zooming on *gla* mRNA levels is depicted below. **(B)** Specific α-Gal A activity in homogenates of developing zebrafish embryos and adult fish organs and tissue, determined as the residual activity towards 4MU-α-Gal after inactivation of α-Nagal activity using 200 mM GalNAc sugar. **(C)** Specific α-Nagal activity determined as activity towards 4MU-α-GalNAc. Activity is measured in technical duplicate of a single biological sample.

Zebrafish α-Gal A can hydrolyse Gb3 *in situ*, but not NBD-Gb3 *in vitro*

In order to study the catalytic features of zebrafish α-Gal A and compare the enzyme to human enzyme, cells without endogenous α-GAL A were generated. Human embryonic kidney (HEK293T) cells were mutated in the human *GLA* gene using CRISPR/Cas9 technology and deficient cells were grown from single cell cultures. Two cell populations showed no endogenous human α-GAL A protein upon ABP labelling and subsequent immunoblotting with a specific human α-GAL A antibody (**Figure 7A**). Next, human α-GAL A and zebrafish α-Gal A enzymes were expressed in the established *GLA* knockout (KO) cells under the CMV promoter and at 37 °C. Expression of both α-GAL A enzymes restored activity towards the artificial substrate 4MU-α-Gal (**Figure 7B**). No hydrolysis of the fluorescent NBD-Gb3 lipid was detected in lysates of untransfected cells (#4 in **Figure 7C**), while expression of human α-Gal A restored hydrolysis of NBD-Gb3 into NBD-LacCer (**Figure 7C**). Interestingly, cell lysates containing zebrafish α-Gal A showed no formation of NBD-LacCer from NBD-Gb3, indicating that the fish enzyme is not able to hydrolyse the fluorescent Gb3 substrate, while at the same time its activity towards 4MU-α-Gal is high.

As final part of this study, corrections of the endogenous glycosphingolipids were studied in unmodified HEK293T (wildtype, WT), *GLA* KO cells and *GLA* KO cells transiently expressing human α-GAL A or zebrafish α-Gal A. Levels of Gb3 were increased in the *GLA* KO cells and Gb3 levels were corrected to WT levels in both the human α-GAL A expressing cells as well as the zebrafish α-GAL A expressing cells (**Figure 7D**). These pilot findings indicate that the zebrafish α-GAL A is able to hydrolyse the natural substrate Gb3 in the cellular conditions.

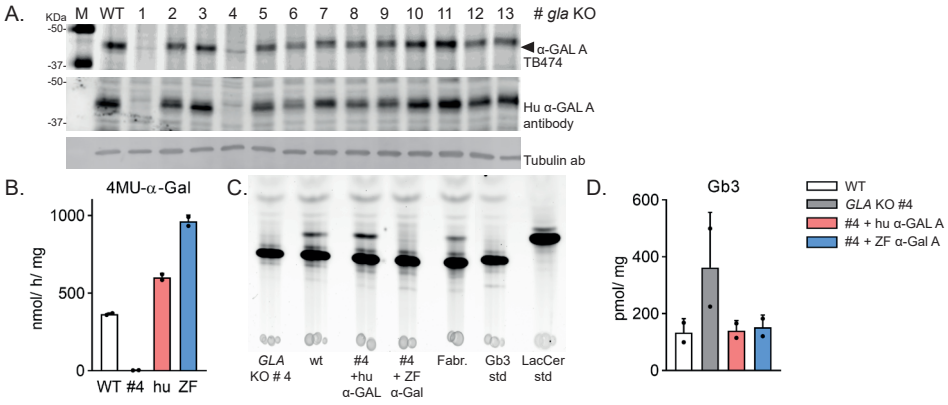

Figure 7 | Catalytic features of human and zebrafish α-GAL A in *GLA* KO cells

(A) Homogenates of unmodified HEK293T cells and various single cell populations after CRISPR/ Cas9 mediated mutagenesis in the *GLA* gene, were labelled with α-Gal configured ABP (top panel, TB474, 1μM) to visualize active enzyme, while all human α-GAL A protein was subsequently detected using an antibody (middle panel). α-tubulin was used as protein loading control (bottom panel). Cell populations # 1-2 were obtained using px335-sgRNA1+sgRNA2, #3-6 using px330-sgRNA1 and #7-13 using px330-sgRNA2. **(B)** Activity towards 4MU-α-Gal in homogenates of unmodified HEK293T cells and *GLA* KO cells as well as *GLA* KO cells expressing human α-GAL A or zebrafish α-Gal A. **(C)** Hydrolysis of NBD-Gb3 by the different cell homogenates and subsequent separation of NBD-lipids by HPTLC using $CHCl_3$/MeOH/15 mM $CaCl_2$ (60/35/8 (v/v/v)). NBD-Gb3 and NBD-LacCer are used as standards. **(D)** Endogenous Gb3 levels in WT cells, *GLA* KO cells and *GLA* KO cells expressing human α-GAL A or zebrafish α-Gal A in pmol/mg. Lipids are measured from two independent transfections in technical duplicate.

Discussion

The zebrafish is a popular research model to study genetic disorders such as lysosomal storage diseases. The CRISPR/Cas9 technology described in this thesis enables efficient generation of zebrafish disease models and is used in previous chapters to evaluate the impact of GBA2 or acid ceramidase defects in the zebrafish Gaucher disease model. A present challenge is to generate a zebrafish model of Fabry disease that is caused by deficiency of α-galactosidase activity. The present study focused on evaluating the presence of endogenous GLA-like α-galactosidase in zebrafish in order to establish whether a Fabry disease zebrafish model is feasible. One orthologue of human α-GAL A and one orthologue of human α-NAGAL was found using an *in silico* BLAST. The presence of zebrafish α-Gal A and α-Nagal was experimentally confirmed in zebrafish materials using α-Gal configured ABPs. The two enzymes contain N-linked glycans and a very similar molecular weight using SDS-PAGE. Next, chemical proteomics was used to detect specific peptides of α-Gal A and α-Nagal to confirmed the presence of both proteins. In this manner both enzymes were detected at protein level in the zebrafish cells, while only α-Gal A could be identified in the fish larvae. Specific mRNA transcripts of *gla* and *naga* were detected in developing zebrafish and various adult tissues as well as activity towards the artificial substrates 4MU-α-Gal and 4MU-α-GalNAc in these materials.

Although α-Gal configured cyclophellitol aziridine inhibitors blocked the activities of α-galactosidase enzymes in zebrafish cells and developing larvae, no accumulation of relevant glycosphingolipids, such as Gb3, was observed. In fact, Gb3 was not detectable in any of the measured zebrafish materials, including those with relatively high *gla* expression and activity towards 4MU-α-Gal. The apparent absence of the glycosphingolipid Gb3 in zebrafish materials, including larvae, brain, liver, kidney, testis and ovary, warrants discussion. Lactosylceramide 4-α-galactosyltransferase (A4GALT) is a member of the glucosyltransferase 32 (GT32) family and the enzyme mediating transfer of an α-galactose moiety from UDP-α-D-galactose to β-D-galactosylceramide, β-D-galactosyl-1,4-β-D-glucosylceramide (lactosylceramide)[23,24]. No protein orthologue of human A4GALT was found using a protein BLAST and no *a4galt* gene is annotated in the zebrafish genome. An orthologue of human A4GALT is also absent in other ray-finned fish species, such as *Oryzias latipes* (medaka) and salmon. Orthologues are present in *Drosophila melanogaster* and *Xenopus tropicalis* (**Supplementary Figure 7**). The only fish species with a known A4GALT orthologue is the coelacanth, the oldest living lineage of Sarcopterygii. The coelacanth is a translational species between fish and tetrapods being more related to lungfish and tetrapods than to ray-finned fish[25].

A number of possible explanations can be considered for the presence of an α-Gal A-like enzyme in zebrafish that apparently lack endogenous Gb3. Firstly, it may mediate intestinal degradation of exogenous oligosaccharides and glycosphingolipids from incoming food. Glycosphingolipid analysis of various food sources was inconclusive about the presence of Gb3. A lipid with similar LC-MS/MS parameters as Gb3 was detected, however the retention time was quite different (**Supplementary Figure 5B**).

Secondly, the enzyme might play a role in turnover of other types of molecules with an α-galactosyl moiety such as polysaccharides composed of one or more α-1,6-linked galactose moieties including plant-derived melibiose, raffinose and stachyose[26]. Nonetheless, these oligosaccharides are not hydrolysed by the intraluminal or intestinal enzymes of humans or other monogastric animal. Instead they are hydrolysed by α-galactosidases of bacteria in the lower small intestine and colon, which produce gas and short-chain fatty acids, such as acetic, propionic and butyric acids[27]. Several publications report on the expression and characterization of α-galactosidases from different sources, including bacteria[28], microspora[29], mushroom[30] and plants[11], not only to treat Fabry disease but also for applications in the food and feed industry[26]. Limited information is available about the intraluminal and intestinal enzymes of digestive tract of zebrafish, only that their intestine consists of one long tube without a distinct stomach, small intestine or large intestine[31]. Finally, specific *gla* mRNA expression and α-Gal A activity was high in the reproductive organs, liver and kidney of the zebrafish, corresponding to high RNA and protein expression in the same tissues of humans[32]. In contrast, the zebrafish intestine showed relatively low α-Gal A activity.

Investigated were also other glycosyltransferase families able to transfer galactose using another glycosidic linkage besides the described α-1,4-linkage mediated by A4GALT (GT32) and the α-1,6-linkage of the raffinose family. In the GT6 family, several globoside α-1,3-N-acetylgalactosaminyltransferases (Forssman synthase-like) are annotated in the zebrafish genome (Gbgt1l1 (Uniprot accession Q7ZTV7), Gbgt1l2 (B0R0W5), Gbgt1l3 (A2CED1), Gbgt1l4 (Q7SXD8)), and one possible α-1,3-galactosyltransferase[33]. However, at present it is unknown whether this annotated ABO blood group transferase (transferase A, α-1,3-N-acetylgalactosaminyltransferase; transferase B, α-1,3-galactosyltransferase; Uniprot code B0S7I1) encodes a functional enzyme and whether active enzymes could have both A (α-1,3-GalNAc) or B (α-1,3-Gal) activity, depending on the sequence, as in humans[3]. Another member of the GT6 family is isogloboside 3 synthase (iGb3S, also called A3GALT), which is reported to transfer an α-1,3-galactosyl moiety to LacCer, generating iGb3[34]. Even though orthologues of iGb3S are annotated in other fish, such as *Oryzias latipes*, no orthologue is documented in the zebrafish genome[33].

Thus, the presence and role of α-Gal A in zebrafish larvae and adult organs remains elusive. No Gb3 is detected using LC-MS/MS techniques nor an orthologue of A4GALT or iGb3S is found in the zebrafish. However, the presence and activity of α-Gal A in zebrafish larvae and distinct adult organs could indicate towards an additional role of α-Gal A besides the hydrolysis of Gb3, α-1,4-galactosyl or α-1,3-galactosyl modified glycoconjugates mediated by A4Galt or iGb3S respectively. On the other hand, the α-Gal A enzyme could have been evolutionary pressured to be present and functional in order to hydrolyse α-Gal containing lipids and proteins of non-endogenous invaders such as bacteria and viruses.

For future endeavours, a zebrafish knockout of *gla* might be useful to study clinical manifestation in the absence of the well-known substrate Gb3 and thereby investigate potentially unknown roles of α-Gal A. Only a few animal disease models for Fabry disease have been developed which are all limited to rodents. Male Fabry mice show a modest to large increase in Gb3 in different tissues, but display no renal complications, only mild myocardial alterations, no spontaneous vascular manifestation and decreased sensitivity to painful stimuli[35-37]. Fabry rats showed accumulation of α-galactosyl glycosphingolipids in serum, dorsal root ganglia, kidney and heart tissue as well as renal tubule dysfunction, mitral valve thickening and neuropathic pain[38,39].

In addition, it would be of great interest to introduce the ability to synthesize the lipid Gb3 in zebrafish. This would allow investigation of the impact of Gb3 by itself as well as Gb3 accumulation during α-Gal A deficiency. In view of this consideration, it was essential to confirm the ability of zebrafish α-Gal A to hydrolyse the substrate Gb3. For this purpose, *GLA* KO HEK293T cells were generated using CRISPR/Cas9 technology and subsequent expression of zebrafish α-Gal A in these cells enabled the study of its catalytic features. Interestingly, expression of zebrafish α-Gal A in the established *GLA* KO cells showed a high *in vitro* activity towards 4MU-α-Gal, but no hydrolysis of the fluorescent NBD-Gb3 lipid was observed. When sensitive LC-MS/MS methods were used to quantify the endogenous Gb3 levels in the different cells, it became apparent that zebrafish α-Gal A was able to correct the increased Gb3 levels of the *GLA* KO cells to WT levels similar to human α-GAL A. These findings indicate that zebrafish α-Gal A is able to hydrolyse endogenous Gb3 *in vivo*. Apparently, the NBD tagged Gb3 does not fit the active site of the zebrafish enzyme or the enzyme requires specific additives in order to be active towards lipid substrates *in vitro*.

In principle, it should be feasible to insert the human *A4GALT* gene in the zebrafish genome using the Tol2 transposon technique, as performed in chapter 4 for human *GBA*. It could be evaluated whether such transgenic fish produce Gb3 and whether their endogenous α-Gal A is able to hydrolyse this *in vivo*. If successful, Gb3-producing Fabry zebrafish (huA4GALT:*gla* KO) could be generated and crossed with *asha1b* KO fish. In this manner Fabry fish could be generated that are unable to form lysoGb3 during α-Gal A deficiency. In analogy to the study on GlcSph in chapter 6, meticulous comparison of Fabry zebrafish with excessive lysoGb3 and those without lysoGb3 will further clarify the postulated toxic action of lysoGb3 in Fabry disease.

Acknowledgements

Kateryna Bila is kindly acknowledged for major contributions to the experimental data in this chapter. Kimberley Zwiers is acknowledged for her contribution on the alignments of zebrafish and human enzymes, Kassiani Kytidou for her input on generating the *GLA* KO cells by CRISPR/Cas9, Rolf Boot for the design of sgRNA sequences and Claire de Wit for her contribution on the characterization of the *GLA* KO HEK293T cells and transient expression of α-GAL A.

Supplementary Figures

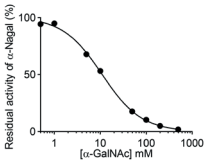

◀ Supplementary Figure 1 | IC_{50} curve of GalNAc (NAGA)
Homogenate of zebrafish larvae was incubated with a range of α-GalNac concentrations (1-500 mM final concentration) and residual activity of α-Nagal was measured using the fluorogenic substrate 4MU-α-GalNAc in technical duplicate.

Supplementary Figure 2 | Structures of used α-Gal configured inhibitors and ABP ▶

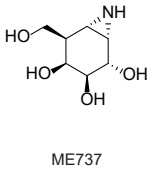

ME737

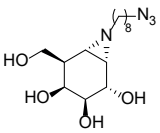

ME739

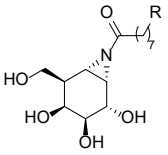

R= Cy 5 (TB474)
R= biotin (ME741)

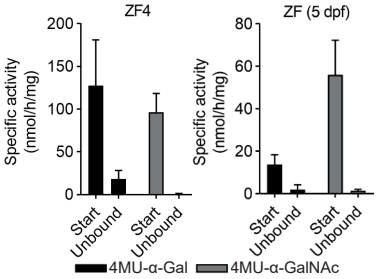

◀ Supplementary Figure 3 | Activity before and after ConA binding.
Activity towards 4MU-α-Gal and 4MU-α-GalNAc was measured of homogenate of zebrafish cells (ZF4) and 5 dpf zebrafish larvae (ZF) before Concanavalin A enrichment (Start) and of the unbound fraction. Activity was measured in technical duplicate.

Supplementary Table 1 | Detected peptide sequences with a score higher than 5.0 (PLGS software) or 25 (Mascot software). The '.' indicates the position of trypsin digestion and the peptide sequence within the two '.' is found. ND = not detected

		Peptide sequence			Peptide sequence
ZF4 cells	**α-Gal A:** F1Q5G5	R.LAVAVMNR.Q K.LADYVHSK.G K.LGIYADVGTK.T K.KLADYVHSK.G K.TFADWGVDLLK.F K.QIIAINQDPLGK.Q R.NYGDVYDQWTSVK.S K.TCAGYPGSLGYYDIDAK.T	ZF4 cells	**A-Nagal A:** A0A0R4IJL2	R.LSEDGWK.E K.GASALVFFSR.R K.AVISNQDPLGIQGR.R R.GIPHLAQYVHDR.G
5 dpf ZF	**α-Gal A:** F1Q5G5	K.SILDWTAEK.Q R.NYGDVYDQWTSVK.S R.LAVAVMNR.Q K.QIIANQDPLGK.Q K.SILDWTAEK.Q K.LGIYADVGTK.T	5 dpf ZF	**A-Nagal A:** A0A0R4IJL2	ND

```
ZF α-Gal A      MRASIIVVIGLVCLLVPAAALDNGLALTPTMGWLHWERFMCNTDCDADPQNCIREELFMQ 60
ZF α-Nagal      MWSA---CVLFLAFSSAALALDNGLMRTPPMGWLAWERFRCDIDCQNDPYNCISEQLFMD
                * ::    : ::.:   * ******  ** **** **** *: **: ** *** *:***:

ZF α-Gal A      MADVMVKEGWKDAGYEFVCIDDCWPSQQRDAQGRLQADPKRFPSGIKKLADYVHSKGLKL 120
ZF α-Nagal      MADRLSEDGWKELGYVYVNIDDCWSSKDRDAQGRLQPDPKRFPRGIPHLAQYVHDRGLKL
                *** : ::***: ** :* ***** *::******** ****** ** :**:***.:****

ZF α-Gal A      GIYADVGTKTCAGYPGS-LGYYDIDAKTFADWGVDLLKFDGCFMPDWHQLGEGYINMSSA 179
ZF α-Nagal      GIYGDMGTLTCGGYPGTTLDKIETDAQTFADWGIDMLKLDGCYSNSS-YQEQGYPMMSKA
                ***.*:** **.****: *.  : **:******:*:**:***:  .     :**  **.*
                          #  #
ZF α-Gal A      LNQTGRSIVYSCEWPLYEWQH-QQPDYEAIRKTCNHWRNYGDVYDQWTSVKSILDWTAEK 238
ZF α-Nagal      LNATGRPIGYSCSWPAYQGGLPPKVNYTLLGQICNLWRNYDDIQDSWDSVMGIVDWFFDN
                ** *** * ***.** *:     : :*  : : ** ****.*: *.* ** .*:**  ::

ZF α-Gal A      QKIVVPVAGPGGWNDPDMLIIGNFGLSRDQQQTQMALWAIMAAPLLMSNDLRDICPKAKE 298
ZF α-Nagal      QDALQPAAAPGQWNDPDMLIIGDFSLSLDQSRAQMALWSIMAAPLFMSNDLRTISSAARS
                *. : *.*.** **********:*.** **.::*****:******:****** *.  *:.

ZF α-Gal A      LLQNKQIIAINQDPLGKQGYRILKAD-SFELWERPLSGNRLAVAVMNRQEIGGPRRFTIS 357
ZF α-Nagal      VLQNKAVISINQDPLGIQGRRLLKEKSGIQVFQRPLSKGASALVFFSRRS-DMPYRYTTS
                :**** :*:******* ** *:** . .:::::**** .  *:..:.*:. . * *:* *

ZF α-Gal A      VAIMPSWKLCNPKCNVTQIMPTYKEMGVQNL--LSEVVVQVNPTGTTLLTVNPL------ 409
ZF α-Nagal      LKTLG------YQPGVFEVFDVFSEQRLPELKDSTQFTVSINPSGVVMWYIYPAADRRKE
                :  :        : .* ::: .:.*  : :*   ::..*.:**:*..:  : *

ZF α-Gal A      ----------------------------
ZF α-Nagal      AEFEGFSKKLIGPKFHRHANEVDAPLVL
```

Supplementary Figure 4 | Alignment of zebrafish α-Gal A with zebrafish α-Nagal.
The amino acid sequences of the pro-protein of zebrafish α-Gal A (Uniprot F1Q5G5) and zebrafish α-Nagal (Uniprot A0A0R4IJL2) were aligned using Clustal Omega[20]. * indicates a conserved residue, : a similar residue. The signal peptide is predicted using SignalP-5.0[21] and depicted in purple. The catalytic Asp residues are depicted in red, the cysteine residues forming disulfide briges in orange and residues interacting and stabilizing the α-galactose in blue. The Glu and Leu residues of α-Gal A and Ser and Ala residues of α-Nagal, which form specificity of the α-galactose of N-acetylgalactosamine moiety are emphasized with #. Specific peptides sequences, obtained from PLGS or Mascot analysis after chemical proteomic, as described in the result section, are underlined in black for α-Gal A and in red for α-Nagal respectively.

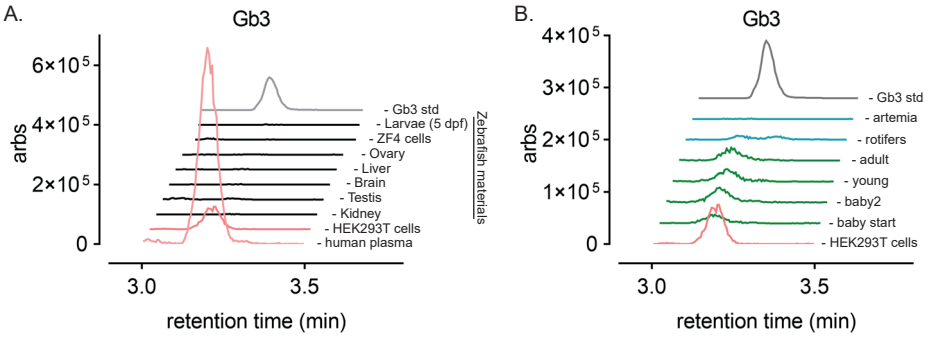

Supplementary Figure 5 | Detection of Gb3 in various samples using LC-MS/MS
(A) Glycosphingolipids were extracted of different human and zebrafish materials and the presence of deacylated Gb3 (784.4>282.3, parent> daughter) was detected and visualized. Two human sources were used as controls (pink lines): 25 µL human plasma and 20 µg of HEK293T WT cell homogenate. Zebrafish homogenates were used of various samples (15 µg protein): kidney, testis, brain, liver, ovary, zebrafish embryonic cells (ZF4) and 5 dpf zebrafish larvae (black lines). **(B)** Lipids of various food sources were also extracted and a peak with the correct parent/daughter was observed in manufactured, plant-based food (green lines), however it is unclear if this signal is actually Gb3. The signal of an extracted equivalent of Gb3 (4 pmol) was used as standard in both figures (grey line).

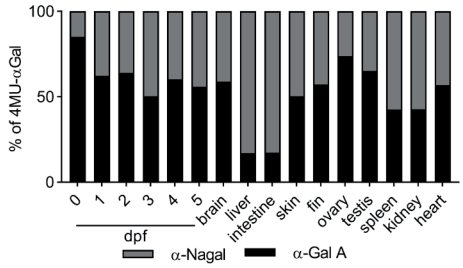

Supplementary Figure 6 | Specific activity of α-Gal A
The activity towards 4MU-α-Gal was measured of homogenates of zebrafish of different ages (t = 0-5 dpf) and various adult organ tissues with and without the presence of 500 mM α-GalNac to inhibit the endogenous α-Nagal enzyme. The hydrolytic activity of α-Nagal towards 4MU-α-Gal was determined and depicted as ratio of the total activity towards 4MU-α-Gal. The specific α-Gal A activity was determined as the residual activity towards 4MU-α-Gal with 500 mM α-GalNac inhibitor and subsequently used in Figure 6B.

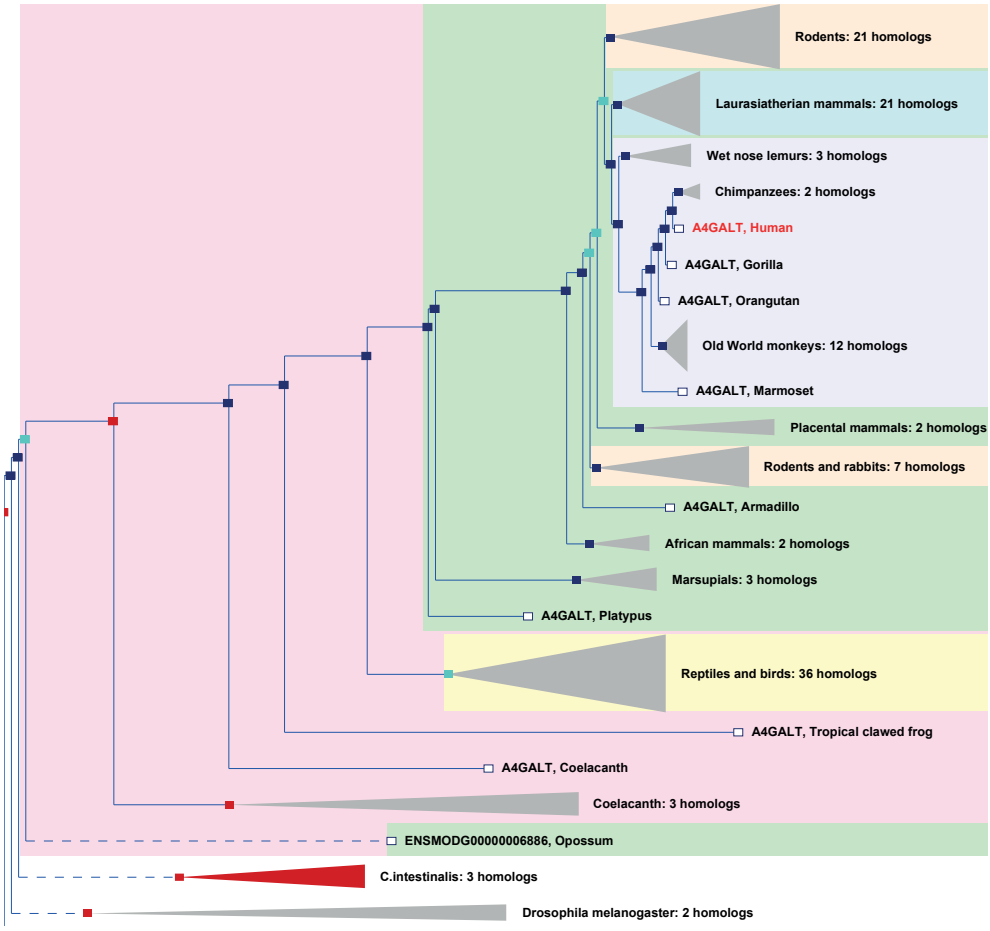

Supplementary Figure 7 | Gene tree of A4GALT
Phylogenetic (gene) tree displaying annotated orthologues of human A4GALT. No ray-finned fish species are depicted in this gene tree. Figure is obtained and exported from Ensembl.

Experimental procedures

Chemicals and reagents - The α-Gal specific inhibitors (ME737 and ME739), ABPs (TB474 and ME741) and C17-dihydroceramide were synthesized at Leiden University (the Netherlands) as reported[16,40]. Chemicals were obtained from Sigma-Aldrich (St. Louis, MO, USA) if not otherwise indicated. LC-MS grade methanol, 2-propanol, water, formic acid and HPLC grade chloroform were purchased from Biosolve (Valkenswaard, the Netherlands). Butanol and hydrochloric acid were obtained from Merck Millipore (Billerica, USA). 4-Methylumbelliferyl 2-acetamido-2-deoxy-a-D-galactopyranoside (4MU-α-GalNAc) was purchased from Carbosynth (Compton, UK), N-Dodecanoyl-NBD-ceramide trihexoside (NBD-C12-Gb3) from Matreya (State college, USA) and C12-NBD Lactosyl Ceramide from Avanti. Primers were ordered from Integrated DNA technologies (IDT; Coralville, USA) without additional purification.

Zebrafish husbandry and samples - Wild-type (WT) zebrafish (ABTL) were a mixed lineage of WT AB and WT TL genetic background. Zebrafish were housed and maintained at Leiden University (the Netherlands) according to standard protocols. The breeding of fish lines was approved by the local animal welfare committee (Instantie voor Dierwelzijn) of Leiden University and followed the international guidelines specified by the EU animal Protection Directive 2010/63/EU. Experiments using embryos and larvae were performed before the free-feeding stage, not falling under animal experimentation law according the EU animal Protection Directive 2010/63/EU. Embryos and larvae were grown in egg water (60 µg/mL Instant Ocean Sera MarinTM aquarium salts (Sera; Heinsberg, Germany)). No adult zebrafish were used for experimentation and organs used in experiments were only obtained from defined old and excess WT zebrafish (> 1.5 years). Animal caretakers killed the WT zebrafish according to in-house protocols, after which organs were dissected from the dead zebrafish. Organs were snap frozen for protein analysis or stored in RNAlater (Invitrogen, ThermoFisher Scientific, Waltham USA) for RT-qPCR analysis and stored at -80 °C.

Cloning - Design of cloning primers and single-guide RNA sequences (sgRNA) were based on NCBI sequences NM_000169 for human *GLA* and NM_001006103 for zebrafish *gla*. The coding regions were amplified using Phusion HighFidelity PCR mastermix (Thermo Fisher Scientific, Waltham, USA) with cDNA as template (in-house human cDNA library or cDNA from extracted 5 dpf zebrafish larvae) using the primers given in **Supplementary Table 2**. Fragments of human and zebrafish *GLA* were cloned into the pDONR vector using GATEWAY™ recombination cloning technology (BP reaction, Thermo Fisher) according to the manufacturer's protocol and sequenced before shuttling the *GLA* fragments to the pDEST-zeo expression vector (derived by replacing the neomycin selection marker in the pDEST vector with a zeomycin selection marker) using the LR reaction. Several pDONR constructs were sequenced with the zebrafish *gla* insert and the insert with the least amount of mutations compared to NM_001006103 was used (**Supplementary Figure 8**). For CRISPR/Cas9 mediated *GLA* targeting in HEK293T cells, sgRNA sequences, given in **Supplementary Table 2**, were cloned into the BbsI restriction site of the px330-U6-chimeric_BB-CB-hSpCas9 vector (Addgene plasmid #42230) or the px335-U6-Chimeric_BB-CBh-hSpCas9n vector (Addgene #42335) for SpCas9 nickase expression. All plasmids were isolated from transformed DH5α cells using a plasmid isolation kit (Qiaprep spin Miniprep kit; Qiagen, Hilden, Germany) and sequenced using Sanger sequencing (Macrogen, Leiden, The Netherlands).

Supplementary Table 2 | List of oligonucleotide sequences.

Primer	Sequence (5' -3')	Purpose
Hu *GLA* sgRNA1 F	caccgTTGTCCAGTGCTCTAGCCCC	sgRNA: px330/335
Hu *GLA* sgRNA1 R	aaacGGGGCTAGAGCACTGGACAAc	sgRNA: px330/335
Hu *GLA* sgRNA2 F	caccgTTGGCAAGGACGCCTACCAT	sgRNA: px330/335
Hu *GLA* sgRNA2 R	aaacATGGTAGGCGTCCTTGCCAAc	sgRNA: px330/335
Human *GLA* F	GGGGACAAGTTTGTACAAAAAAGCAGGCTACCACCATGCAGCTGAGGAACCCAGA	Gateway cloning
Human *GLA* R	GGGGACCACTTTGTACAAGAAAGCTGGGTCTTAAAGTAAGTCTTTTAATGACATC	Gateway cloning
Zebrafish *gla* F	ggggacaagtttgtacaaaaaagcaggcttcaccaccATGCGTGCCTCAATTATAGTC	Gateway cloning
Zebrafish *gla* R	ggggaccactttgtacaagaaagctgggtcCAGTGGGTTGACGGTGAGTAG	Gateway cloning

Cell culture and transfection - Zebrafish embryonic fibroblasts (ZF4 cells[41]) were cultured at 28 °C and 5% CO_2 in DMEM/F12 medium, supplied with 10% (v/v) Fetal Calf Serum, 0.1% (w/v) penicillin/streptomycin, and 1% (v/v) Glutamax. HEK293T cells were cultured at 37 °C and 5% CO_2 in DMEM medium, supplied with 10% (v/v) FCS, 0.1% (w/v) penicillin/streptomycin and 1% (v/v) Glutamax. HEK293T *GLA* KO Cells were obtained by transfecting HEK293T cells seed in 6-well plates with the px330-*GLA* construct (px330-*GLA*-sgRNA1 or px330-*GLA*-sgRNA2) or both px335-*GLA* constructs (sgRNA1+sgRNA2) in combination with PEI (PEI/DNA, 3/1 (w/w)). After 72 hours, cells were diluted to approximately 0.5 cell/ well, seeded in 96-well plates and individual clones were cultured over the next weeks. Activity towards 4MU-α-Gal was determined as well as ABP labelling as described in the result section and the two clones (#1 and #4) without residual activity and ABP-labelled protein were maintained. *GLA* KO clone 4 was used for subsequent experiments and further mentioned as *GLA* KO cells. *GLA* KO cells were transfected using PEI and the pDEST-zeo-*GLA* construct (PEI/DNA, 3/1 (w/w)) and incubated for 72 hours before harvesting. In general, HEK293T cells were harvested by pipetting in PBS, while ZF4 cells were harvested using trypsin (0.25% (v/v) trypsin in PBS, no EDTA). Cell pellets were washed twice with PBS and stored at -80 °C until use.

Homogenate preparation - Cell homogenates were prepared in potassium phosphate (Kpi lysis buffer, supplemented with Triton-X100 and benzonase (25 mM K_2HPO_4-KH_2PO_4, pH 6.5, 0.1% (v/v) Triton-X100 and 25 U/mL benzonase) and lysed using sonication (20% amplitute, 3s on, 3s off for 4cycles) while on ice. Whole zebrafish embryos or larvae or zebrafish organs were resuspended in Kpi lysis buffer (12.5 µL/embryo, 100 µL for small organs (spleen, kidney, heart, fin) or 200-400 µL for larger organs (brain, liver, intestine, skin), supplemented with 0.1% Triton-X100 and EDTA-free protease inhibitor (25 mM K_2HPO_4-KH_2PO_4, pH 6.5, 0.1% (v/v) Triton-X100 an 1x cOmplete™, EDTA-free Protease Inhibitor Cocktail, Roche, Bazel, Switzerland). Embryos and organs were first homogenized using a Dounce homogenizer (10 strokes), followed by sonication as described. Total protein concentration of homogenates was determined using Pierce™ BCA protein assay kit (ThermoFisher Scientific) and measured using an EMax® plus microplate reader (Molecular Devices, Sunnyvale, USA). Homogenates of organs were stored at -80 °C, homogenates with a protein concentration higher than 5 mg/mL were diluted with KPi lysis buffer and stored in aliquots.

Enzyme activity assay

General assay procedures - Generally assays were performed using homogenate in KPi (12.5 uL, 12.5-50 µg total protein) by addition of McIlvaine (citric acid – Na_2HPO_4) buffer of the appropriate pH (12.5 uL; 150 mM McIlvaine pH4) and supplemented with a covalent inhibitor if mentioned, before addition of 4-methylumbelifferone (4MU-aglycone) mixes; 100 µL of 3.75 mM 4-MU α-D-galactopyranoside (4MU-α-Gal) substrate with 0.1% (w/v) Bovine Albumin Serum (BSA) or 100 µL of 1 mM 4-MU α-D-N-acetylgalactoside (4MU-α-GalNAc) substrate. Incubation was performed at 37 °C for 30 min for ZF4 cells and 60 min for zebrafish embryos or organs unless indicated otherwise and stopped by addition of glycine-NaOH STOP buffer (200 µL; 1 M Glycine-NaOH, pH 10.3). All activity assays were measured using a LS-55 (PerkinElmer, Waltham, USA; λ_{ex} of 366 nm, λ_{em} of 445nm) and calculated using a standard of 1 nmol 4MU.

α-Nagal activity was blocked by addition of the sugar α-N-acetyl-galactosaminide (α-GalNAc; NAGA), with a final concentration of 200 mM in the assay (concentration in substrate mix: 250 mM NAGA). For the zebrafish embryo and larvae samples, a homogenate without substrate mix was included and used as blanc to account for background fluorescent signal originating from the sample. All activities were measured using 3 independent homogenates measured in technical duplo unless indicated otherwise in the result section.

pH curves - PH curves were obtained by incubating homogenate (12.5 uL, ± 12.5 ug total protein) with McIlvaine of the appropriate pH (62.5 uL; 300 mM McIlvaine, pH 2-8) on ice for 5 minutes before addition of two-times concentrated 4MU-α-Gal or 4MU-α-GalNAc substrate mix (50 uL; 7,5 mM 4MU-α-Gal or 2 mM 4MU-α-GalNAc, 0.2% (w/v) BSA in MilliQ).

IC_{50} measurements - For the covalent α-Gal configured inhibitors, homogenate (12.5 µL, ± 12.5 µg total protein) was pre-incubated with the inhibitor (2x concentrated in 300mM McIlvaine pH 4 with 1% (v/v) DMSO; final concentration of 0.5% (v/v) DMSO and 0.001- 100 µM for ME737 and ME739, 0.0001- 50 µM for TB474) for 1 h at 37 °C, before addition of 100 µL 4Mu-α-Gal or 4MU-α-GalNAc substrate mix and incubation as described in the general assay procedures. IC_{50} values were calculated using Graphpad Prism (v8.1.1, GraphPadsoftware, CA, USA).

Activity-based probe (ABP) labelling and chemical proteomics

General ABP labelling procedure - Zebrafish cell, embryo or organ homogenate (10 µL, xxx µg total protein) was labelled with the α-Gal configured ABP TB474 (2 µM TB474 in 10 µL 300 mM McIlvaine buffer pH 4, 1% (v/v) DMSO; final concentration of 1 µM TB474 and 0.5% (v/v) DMSO) for 30 min at 37 °C. For the inhibitor experiment, zebrafish α-Gal and Nagal were preblocked by incubating homogenate (10 µL) with α-Gal configured inhibitor ME737 (100 µM in 10 µL 300 mM McIlvaine buffer pH 4, 1% (v/v) DMSO; final concentration of 50 µM and 0.5% (v/v) DMSO) for 30 min at 37 °C before the addition of TB747 (3 µM TB474 in 10 µL 300 mM McIlvaine buffer pH 4, 1% DMSO; final concentration of 1 µM TB474 and 0.5% (v/v) DMSO). Proteins were denatured with 5x Laemmli sample buffer (25% (v/v) 1.25 M Tris-HCl pH 6.8, 50% (v/v) 100% glycerol, 10% (w/v) sodium dodecyl sulfate (SDS), 8% (w/v) dithiothreitol (DTT); and 0.1% (w/v) bromophenol blue) and boiled for 5 min at 98 °C. ABP-labelled protein samples were separated by electrophoreses on 10% (w/v) SDS-PAGE gels, before scanning the fluorescence of the wet-slab gel with a Typhoon FLA 9500 (GE Healthcare, Chicago, USA; Cy5 (λ_{EX} of 635 nm, λ_{EM} of 665 nm), 750 V, pixel size 100 µm). Gels were stained with Coomassie Brilliant Blue staining (CBB-G250) and scanned on a ChemiDoc™ MP imager (Bio-Rad; Hercules, USA). For western blotting, proteins were transferred to a nitrocellulose membrane (0.2 µM, Bio-Rad) using the Trans-blot® Turbo™ Transfer system (Bio-Rad). Membranes were blocked with 5% (w/v) bovine albumin serum (BSA) and incubated overnight at 4 °C with primary antibodies: mouse anti-human α-tubulin (1:10.000; clone DM1A) or rabbit anti-α-Gal A (1:1000; Abnova, Taipai, Taiwan). Membranes were washed 3 times with TBST and incubated with 1 h at RT with complementary secondary antibodies: donkey anti-mouse Alexa 488 (1:10.000; Invitrogen) or GARPO goat anti rabbit IgG (H+L) peroxidase (1:5000, Bio-Rad). Fluorescent signal was detected using a Typhoon, while chemiluminescense signal was detected using a ChemiDoc MP imager.

Deglycosylation using PNGase F - Glycoproteins were deglycosylated using PNGase F (New England Biolabs, Ipswich, USA) according to the manufacturer's instructions. Briefly, zebrafish cell and larvae homogenate was labelled with TB474, as described above, in 2x volumes (40 µL final volume). After incubation for 30 min at 37 °C, the mixture was denatured using Glycoprotein buffer (supplied) and boiled for 10 min at 98 °C. The sample was divided, NP-40 (supplied) and MQ was added to both samples NP-40 and one 20 µL sample was incubated with PNGase F, while the other 20 µL sample was incubated with MQ for 1 h at 37 °C. Laemmli sample buffer (5x) was added after incubation and the samples were separated on a 10% (w/v) SDS-PAGE gel and scanned as described above.

Chemical proteomics - ZF4 cell and zebrafish 5 dpf embryos homogenate (125 µL; 125 µg total protein) was incubated with biotin-ABP ME741 (5 µM ME741 in 150 mM McIlvaine buffer pH 4; final DMSO concentration of 0.5% and final volume 250 µL) for 2 h at 37 °C. The labelling was stopped by addition of 20 µL 20% (w/v) SDS and subsequent boiling of the sample at 95 °C for 5 min. Proteins were precipitated by chloroform/methanol, proteins were rehydrated in 2% (w/v) SDS in PBS followed by reduction using DTT (final concentration of 5 mM DTT in MQ) for 30 min at 45 °C and alkylation using iodacetamide (final concentration of 15 mM in MQ) for 30 min at RT in dark. Another chloroform/methanol precipitation was performed, proteins were rehydrated in 2% (w/v) in PBS buffer and ABP-bound proteins were enriched by incubation with paramagnetic avidin beads (Dynabeads™ MyOne™ Strptavidin T1, Thermo Fisher Scientific) at 4 °C overnight. Beads were washed with 0.1% (w/v) SDS in PBS, 2x with PBS, 1x with 4 M urea in 50 mM NH_4HCO_3 followed by a wash with PBS and 2x MQ. On-bead tryptic digestion was performed by incubating the beads in trypsin digestion buffer (100 µL, 2.5 ng/µL trypsin in 50 mM NH_4NO_3, pH 8 with 2% (v/v) CAN and 1 mM $CaCl_2$) overnight at 37 °C with shaking. Prior to LC-MS analysis, peptides were desalted by Stagetips prepared using Empore™ C18 47-mm extraction discs[42]. Samples were analysed on a Synapt G2Si mass spectrometer (Waters, Milford, USA) operating with Masslynx for acquisition as previously described[43], proteins were identified using the *Danio rerio* proteome (Uniprot code UP000000437) and either Mascot software or ProteinLynx Global Server (PLGS) was used for peptide identification.

Concanavilin A lectin binding - Concanavalin A-Sepharose 4B beads (ConA beads; Sigma) were first washed three times in 0.1 M sodium acetate, 0.1 M NaCl, 1 mM MgCl2, 1 mM CaCl2, 1 mM MnCl2, pH 6.0, washing buffer using brief centrifugation at 2000 rpm for 2 min. Next, 100 µL of beads were mixed with 100 µL of 4 mg/ml zebrafish or cells lysate. The samples were incubated overnight at 4 °C while rotating. Afterwards, the mixture was centrifuged at 13000 rpm at 4 °C for 10 min. The supernatant was collected, the beads were washed three times with washing buffer and the beads were stored in 100 µL wash buffer. Four fractions were collected: sample prior to ConA beads incubation ('start'), supernatant after incubation with the beads ('unbound'), supernatatant after the third wash ('wash') and beads pellet ('ConA bound'). Afterwards, the fractions were labelled with ABP TB474 and enzyme activity towards 4MU-α-GAL and 4MU-α-GalNAc was measured as described in the general assay procedures. The protein concentrations of the unbound, wash and ConA bound fraction were determined. Instead, the amount of sample for ABP labelling and enzyme activity was the same for the 4 fractions and the specific activity was calculated as nmol/mL sample or depicted as ratio of the start material.

Treatment of cells or embryos with inhibitors - ZF4 cells were transferred to 6-well plates and grown to 70-80% confluency before addition of 1mL fresh culture medium supplemented with vehicle (0.5% (v/v) DMSO) or inhibitor (0.001, 0.01, 1, 5 or 10 µM of ME737 or ME739). Cells were incubated for 24 hours, washed three times with PBS before harvesting the well content on ice by addition of 100 µL ice-cold KPi lysis buffer (25 mM KPi buffer pH 6.5, 0.1% (v/v) Triton X-100 and protease inhibitor) and scraping. The sample is collected, sonicated to obtain a homogenate sample and the total protein was determined using the BCA assay as described before. Using this procedure, the protein concentration of these *in situ* treated cell homogenates was between 1 and 2 mg/mL. Enzyme activity towards 4MU-α-Gal and 4MU-αGalNAc was measured in technical replicate as described in the general assay procedures. Adult WT zebrafish were crossed and developing off-spring (8 h post-fertilization) was incubated in 100 µL egg water immersed with vehicle (0.5% (v/v) DMSO) or inhibitor (20, 50 or 100 µM ME737 or ME739 with 0.5% (v/v) DMSO) for 5 days at 28 °C. Larvae (5 dpf) were washed with egg water and stored in pools of 3 larvae for enzyme activity measurements and single larvae in 2 mL Safe-Lock Eppendorf tubes for glycosphingolipid analysis. Homogenate was prepared by addition of 60 µL KPi lysis buffer, sonication and protein determination was performed as described before. Enzyme activity towards 4MU-α-Gal and 4MU-α-GalNAc was measured in technical replicate as described in the general assay procedures.

Glycosphingolipid analysis – The internal standard C17-dihydroceramide (20 µL, 20 pmol/ µL in MeOH) was added to homogenate (10 µL, 20-50 µg total protein in KPi lysis buffer) and neutral (glyco) sphingolipids were extracted using an acidic Bligh and Dyer procedure (1/1/0.9 chloroform/ methanol/ 100 mM formate buffer pH 3.1) as described before[22,40]. The lower phase was concentrated and lipids were deacylated using sodium hydroxide (0.5 M NaOH in MeOH) in combination with a microwave protocol described before[44]. Samples were neutralized, a butanol/water clean-up was performed and lipids were resuspended in methanol for separation as described before[40].

Hydrolytic activity towards NBD-Gb3 – NBD-C12-Gb3 was concentrated and resuspended in McIlvaine buffer (150 mM McIlvaine buffer pH 4.5, 0.05% (v/v) Triton X-100 and 0.05% (w/v) sodium taurocholate and MQ to a total volume of 60 µL; 5 µM NBD-C12-Gb3 final concentration) before addition of cell homogenate (40 µL, 80 µg total protein) or Fabrazyme (0.18 pmol in 40 µL McIlvaine buffer pH 4.5 with 0.05% (v/v) Triton-X100 and 0.2% (w/v) sodium taurocholate). Samples were incubated for 3 h at 37°C and stopped by addition of MeOH, $CHCl_3$ and MQ to a final ratio of 1/1/0.9 with subsequent Bligh and Dyer extraction. The lower phase was concentrated and lipids reconstituted in $CHCl_3$/MeOH (2/1) and separated by thin layer chromatography on a HPTLC silica gel 60 plate (VWR) using $CHCl_3$/ MeOH/ $CaCl_2$ (60/35/8 (v/v) of $CHCl_3$/MeOH/15 mM $CaCl_2$) as eluent. The HPTLC plate with NBD-lipids was scanned using a Typhoon imaging system (cy2 settings (λ_{ex} of 488 nm, λ_{em} of 515-535 nm), 250 V, pixel size 100 µM.

Gene expression analysis - RNA of organs and zebrafish eggs or larvae (10 eggs or larvae per sample) was extracted using a Nucleospin RNA XS column (Machinery-Nagel, Düren, Germany) according to supplier's protocol, without the addition of carrier RNA. Contaminating DNA was degraded on column by a DNase I treatment (supplied in the kit). cDNA was synthesized using SuperScript™ II reverse transcriptase (Invitrogen, ThermoFisher Scientific, Waltham, USA) using oligo(dT) and an input of approximately 1000 ng total RNA according to the manufacturer's instruction. Generated cDNA was diluted to an approximate concentration of 0.5 ng total RNA input/µL with Milli-Q water. RT-qPCR reactions were performed with the IQ SYBR green mastermix (Bio-Rad) in a total volume of 15 µL (1x SYBR green, 333 µM of forward and reverse primer as given in **Supplementary Table 3** and 5 µL of the diluted cDNA input) and carried out using a CFX96™ Real-Time PCR Detection system (Bio-Rad) with the following conditions: denaturation at 95 °C for 3 min, followed by 40 cycles of amplification (95 °C for 30 sec and 61 °C for 30 sec), imaging the plate after every extension at 61 °C, followed by a melt program from 55-95 °C with 0.5 °C per step with imaging the plate every step. All biological samples were tested in technical duplicate and gene expression was normalized to two house-keeping genes *ef1α* and *rpl13α* and depicted as ΔCt value.

Supplementary Table 3| Forward and reverse primers for RT-qPCR analysis.

Target	Forward primer sequence (5'->3')	Reverse primer sequence (5'->3')	
gla	TCTGGGCAAACAGGGCTAT	GGGTTACGTTGCATTTCGGG	188 bp
naga	TCGCTCCGTCCTCCAGAATA	ATGGCATATCAGACCTGCGG	167 bp
ef1α	CTGGAGGCCAGCTCAAACAT	ATCAAGAAGAGTAGTACCGCTAGCATTAC	Ref. 45
rpl13α	TCTGGAGGACTGTAAGAGGTATGC	AGACGCACAATCTTGAGAGCAG	Ref. 45

```
ATG CGT GCC TCA ATT ATA GTC GTT ATC GGA CTT GTA TGT TTA TTA GTC CCA GCC
M   R   A   S   I   I   V   V   I   G   L   V   C   L   L   V   P   A
GCG GCG CTA GAC AAC GGC CTG GCT TTA ACT CCC ACC ATG GGC TGG CTG CAC TGG
A   A   L   D   N   G   L   A   L   T   P   T   M   G   W   L   H   W
GAG AGA TTC ATG TGC AAC ACA GAC TGT GAT GCG GAT CCT CAA AAC TGC ATT AGA
E   R   F   M   C   N   T   D   C   D   A   D   P   Q   N   C   I   R
GAG GAG CTC TTC ATG CAG ATG GCA GAT GTG ATG GTG AAG GAG GGA TGG AAG GAT
E   E   L   F   M   Q   M   A   D   V   M   V   K   E   G   W   K   D
GCT GGA TAT GAG TTT GTG TGC ATT GAT GAT TGC TGG CCT TCG CAA CAA AGG GAC
A   G   Y   E   F   V   C   I   D   D   C   W   P   S   Q   Q   R   D
GCA CAG GGG CGC CTG CAG GCA GAC CCC AAA AGG TTT CCC AGT GGC ATC AAA AAA
A   Q   G   R   L   Q   A   D   P   K   R   F   P   S   G   I   K   K
CTG GCA GAT TAT GTC CAT TCT AAA GGA CTG AAG CTG GGA ATA TAT GCA GAT GTG
L   A   D   Y   V   H   S   K   G   L   K   L   G   I   Y   A   D   V
GGC ACA AAA ACT TGT GCA GGT TAC CCT GGG AGT TTG GGC TAT TAT GAC ATC GAT
G   T   K   T   C   A   G   Y   P   G   S   L   G   Y   Y   D   I   D
GCA AAA ACC TTT GCG GAC TGG GGT GTG GAT CTG TTA AAA TTT GAC GGG TGT TTC
A   K   T   F   A   D   W   G   V   D   L   L   K   F   D   G   C   F
ATG CCT GAC TGG CAT CAG CTG GGA GAA GGT TAT ATA AAT ATG TCA AGT GCA CTA
M   P   D   W   H   Q   L   G   E   G   Y   I   N   M   S   S   A   L
AAC CAG ACT GGC AGA AGT ATT GTT TAC TCT TGT GAA TGG CCG TTA TAT GAG TGG
N   Q   T   G   R   S   I   V   Y   S   C   E   W   P   L   Y   E   W
CAG CAC CAA CAG CCT GAC TAT GAG GCA ATT CGC AAG ACC TGT AAC CAC TGG CGT
Q   H   Q   Q   P   D   Y   E   A   I   R   K   T   C   N   H   W   R
AAT TAT GGA GAT GTG TAT GAC CAG TGG ACC AGT GTG AAG AGC ATC CTG GAC TGG
N   Y   G   D   V   Y   D   Q   W   T   S   V   K   S   I   L   D   W
ACA GCA GAA AAG CAG AAG ATC GTC GTC CCA GTG GCA GGA CCA GGA GGA TGG AAT
T   A   E   K   Q   K   I   V   V   P   V   A   G   P   G   G   W   N
GAC CCT GAC ATG CTG ATC ATT GGA AAC TTC GGC TTG AGT CGC GAT CAG CAG CAG
D   P   D   M   L   I   I   G   N   F   G   L   S   R   D   Q   Q   Q
ACT CAG ATG GCA TTG TGG GCA ATC ATG GCG GCT CCA CTT CTA ATG TCT AAC GAC
T   Q   M   A   L   W   A   I   M   A   A   P   L   L   M   S   N   D
CTG CGA GAC ATC TGT CCC AAA GCC AAA GAA CTA CTG CAG AAC AAG CAG ATC ATC
L   R   D   I   C   P   K   A   K   E   L   L   Q   N   K   Q   I   I
GCC ATC AAC CAG GAC CCT CTG GGC AAA CAG GGC TAT CGG ATA TTG AAG GCT GAC
A   I   N   Q   D   P   L   G   K   Q   G   Y   R   I   L   K   A   D
AGT TTT GAG CTG TGG GAA AGG CCC TTG TCA GGC AAC AGG CTG GCC GTG GCA GTG
S   F   E   L   W   E   R   P   L   S   G   N   R   L   A   V   A   V
ATG AAC AGA CAG GAG ATT GGA GGT CCG CGC AGA TTT ACT ATT TCG GTG GCA ATA
M   N   R   Q   E   I   G   G   P   R   R   F   T   I   S   V   A   I
ATG CCT AGC TGG AAG CTT TGT AAC CCG AAA TGC AAC GTA ACC CAG ATC CTG CCC
M   P   S   W   K   L   C   N   P   K   C   N   V   T   Q   I   L/M P
ACT TAC AAG GAA ATG GGT GTC CAA AAT CTC TTG TCA GAG GTG ATG GTC CAA GTC
T   Y   K   E   M   G   V   Q   N   L   L   S   E   V   M/V V   Q   V
AAC CCT ACA GGC ACA ACA CTA CTC ACC GTC AAC CCA CTG TGA  < 1230
N   P   T   G   T   T   L   L   T   V   N   P   L   *
```

Supplementary Figure 8 | zebrafish *gla* sequence
The zebrafish gla coding sequence is amplified using zebrafish cDNA as template and cloned into the pDONR vector as described in the experimental procedures. This sequence is obtained from Sanger sequencing of the resulting pDONR-gla. The obtained sequence showed genetic variations resulting in the same amino acid (depicted in orange) compared to the annotated gene (NCBI code NM_001006103), but only one polymorphism resulting in an amino acid substitution (depicted in red, with the NCBI annotated amino acid given after the /).

References

1. Sweeley C.C.and Klionsky B. (1963) Fabry's Disease: Classification as a Sphingolipidosis and Partial Characterization of a Novel Glycolipid. *J Biol Chem* **238**, 3148-3150.
2. Desnick R.J., Ioannou Y.and Eng C.M. (2001) α-Galactosidase A deficiency: Fabry disease. *In The metabolic and Molecular Bases of Inherited Disease*, C.R. Scriver, A.L. Beaudet, W.S. Sly and D. Valle, eds. (New York: McGraw-Hill), pp. 3733-3744.
3. Yamamoto F. (2004) Review: ABO blood group system--ABH oligosaccharide antigens, anti-A and anti-B, A and B glycosyltransferases, and ABO genes. *Immunohematology* **20**, 3-22.
4. Gold H., Mirzaian M., Dekker N., Joao Ferraz M., Lugtenburg J., Codee J.D.,... and Poorthuis B.J. (2013) Quantification of globotriaosylsphingosine in plasma and urine of fabry patients by stable isotope ultraperformance liquid chromatography-tandem mass spectrometry. *Clin Chem* **59**, 547-556.
5. Aerts J.M., Ferraz M.J., Mirzaian M., Gaspar P., Oussoren S.V., Wisse P.,... and Marques A.R.A. (2017) Lysosomal Storage Diseases. For Better or Worse: Adapting to Defective Lysosomal Glycosphingolipid Breakdown. *In eLS*. (John Wiley & Sons, Ltd), pp. 1-13.
6. Ledvinova J., Poupetova H., Hanackova A., Pisacka M.and Elleder M. (1997) Blood group B glycosphingolipids in alpha-galactosidase deficiency (Fabry disease): influence of secretor status. *Biochimica et biophysica acta* **1345**, 180-187.
7. Witte M.D., Kallemeijn W.W., Aten J., Li K.Y., Strijland A., Donker-Koopman W.E.,... and Aerts J.M. (2010) Ultrasensitive in situ visualization of active glucocerebrosidase molecules. *Nature chemical biology* **6**, 907-913.
8. Willems L.I., Beenakker T.J., Murray B., Scheij S., Kallemeijn W.W., Boot R.G.,... and Overkleeft H.S. (2014) Potent and selective activity-based probes for GH27 human retaining alpha-galactosidases. *Journal of the American Chemical Society* **136**, 11622-11625.
9. Marques A.R., Willems L.I., Herrera Moro D., Florea B.I., Scheij S., Ottenhoff R.,... and Aerts J.M. (2017) A Specific Activity-Based Probe to Monitor Family GH59 Galactosylceramidase, the Enzyme Deficient in Krabbe Disease. *Chembiochem* **18**, 402-412.
10. Kuo C.L., van Meel E., Kytidou K., Kallemeijn W.W., Witte M., Overkleeft H.S.,... and Aerts J.M. (2018) Activity-Based Probes for Glycosidases: Profiling and Other Applications. *Methods Enzymol* **598**, 217-235.
11. Kytidou K., Beekwilder J., Artola M., van Meel E., Wilbers R.H.P., Moolenaar G.F.,... and Aerts J. (2018) Nicotiana benthamiana alpha-galactosidase A1.1 can functionally complement human alpha-galactosidase A deficiency associated with Fabry disease. *J Biol Chem* **293**, 10042-10058.
12. Wang A.M.and Desnick R.J. (1991) Structural organization and complete sequence of the human alpha-N-acetylgalactosaminidase gene: homology with the alpha-galactosidase A gene provides evidence for evolution from a common ancestral gene. *Genomics* **10**, 133-142.
13. Schindler D., Bishop D.F., Wolfe D.E., Wang A.M., Egge H., Lemieux R.U.and Desnick R.J. (1989) Neuroaxonal dystrophy due to lysosomal alpha-N-acetylgalactosaminidase deficiency. *N Engl J Med* **320**, 1735-1740.
14. Vandiggelen O.P., Schindler D., Kleijer W.J., Huijmans J.M.G., Galjaard H., Linden H.U.,... and Cantz M. (1987) Lysosomal Alpha-N-Acetylgalactosaminidase Deficiency-a New Inherited Metabolic Disease. *Lancet* **2**, 804-804.
15. Garman S.C.and Garboczi D.N. (2004) The molecular defect leading to Fabry disease: structure of human alpha-galactosidase. *J Mol Biol* **337**, 319-335.
16. Kytidou K., Beenakker T.J.M., Westerhof L.B., Hokke C.H., Moolenaar G.F., Goosen N.,... and Aerts J. (2017) Human Alpha Galactosidases Transiently Produced in Nicotiana benthamiana Leaves: New Insights in Substrate Specificities with Relevance for Fabry Disease. *Front Plant Sci* **8**, 1026.
17. Tajima Y., Kawashima I., Tsukimura T., Sugawara K., Kuroda M., Suzuki T.,... and Sakuraba H. (2009) Use of a modified alpha-N-acetylgalactosaminidase in the development of enzyme replacement therapy for Fabry disease. *Am J Hum Genet* **85**, 569-580.
18. Tomasic I.B., Metcalf M.C., Guce A.I., Clark N.E.and Garman S.C. (2010) Interconversion of the specificities of human lysosomal enzymes associated with Fabry and Schindler diseases. *J Biol Chem* **285**, 21560-21566.
19. Eng C.M., Guffon N., Wilcox W.R., Germain D.P., Lee P., Waldek S.,... and International Collaborative Fabry Disease Study G. (2001) Safety and efficacy of recombinant human alpha-galactosidase A replacement therapy in Fabry's disease. *N Engl J Med* **345**, 9-16.
20. Madeira F., Park Y.M., Lee J., Buso N., Gur T., Madhusoodanan N.,... and Lopez R. (2019) The EMBL-EBI search and sequence analysis tools APIs in 2019. *Nucleic acids research* **47**, W636-W641.
21. Almagro Armenteros J.J., Tsirigos K.D., Sonderby C.K., Petersen T.N., Winther O., Brunak S.,... and Nielsen H. (2019) SignalP 5.0 improves signal peptide predictions using deep neural networks. *Nat Biotechnol* **37**, 420-423.
22. Lelieveld L.T., Mirzaian M., Kuo C.L., Artola M., Ferraz M.J., Peter R.E.A.,... and Aerts J. (2019) Role of beta-glucosidase 2 in aberrant glycosphingolipid metabolism: model of glucocerebrosidase deficiency in zebrafish. *J Lipid Res* **60**, 1851-1867.

23. Kojima Y., Fukumoto S., Furukawa K., Okajima T., Wiels J., Yokoyama K.,... and Furukawa K. (2000) Molecular cloning of globotriaosylceramide/CD77 synthase, a glycosyltransferase that initiates the synthesis of globo series glycosphingolipids. *J Biol Chem* **275**, 15152-15156.
24. Keusch J.J., Manzella S.M., Nyame K.A., Cummings R.D.and Baenziger J.U. (2000) Cloning of Gb3 synthase, the key enzyme in globo-series glycosphingolipid synthesis, predicts a family of alpha 1, 4-glycosyltransferases conserved in plants, insects, and mammals. *J Biol Chem* **275**, 25315-25321.
25. Meyer A.and Schartl M. (1999) Gene and genome duplications in vertebrates: the one-to-four (-to-eight in fish) rule and the evolution of novel gene functions. *Curr Opin Cell Biol* **11**, 699-704.
26. Bhatia S., Singh A., Batra N.and Singh J. (2019) Microbial production and biotechnological applications of alpha-galactosidase. *Int J Biol Macromol*.
27. Gray G.M. (1975) Carbohydrate digestion and absorption. Role of the small intestine. *N Engl J Med* **292**, 1225-1230.
28. Huang Y., Zhang H., Ben P., Duan Y., Lu M., Li Z.and Cui Z. (2018) Characterization of a novel GH36 alpha-galactosidase from Bacillus megaterium and its application in degradation of raffinose family oligosaccharides. *Int J Biol Macromol* **108**, 98-104.
29. Yang D., Tian G., Du F., Zhao Y., Zhao L., Wang H.and Ng T.B. (2015) A Fungal Alpha-Galactosidase from Pseudobalsamia microspora Capable of Degrading Raffinose Family Oligosaccharides. *Appl Biochem Biotechnol* **176**, 2157-2169.
30. Xu L., Chen B., Geng X., Feng C., Meng J.and Chang M. (2019) A protease-resistant alpha-galactosidase characterized by relatively acid pH tolerance from the Shitake Mushroom Lentinula edodes. *Int J Biol Macromol* **128**, 324-330.
31. Menke A.L., Spitsbergen J.M., Wolterbeek A.P.and Woutersen R.A. (2011) Normal anatomy and histology of the adult zebrafish. *Toxicol Pathol* **39**, 759-775.
32. Uhlen M., Fagerberg L., Hallstrom B.M., Lindskog C., Oksvold P., Mardinoglu A.,... and Ponten F. (2015) Proteomics. Tissue-based map of the human proteome. *Science* **347**, 1260419.
33. Turcot-Dubois A.L., Le Moullac-Vaidye B., Despiau S., Roubinet F., Bovin N., Le Pendu J.and Blancher A. (2007) Long-term evolution of the CAZY glycosyltransferase 6 (ABO) gene family from fishes to mammals--a birth-and-death evolution model. *Glycobiology* **17**, 516-528.
34. Keusch J.J., Manzella S.M., Nyame K.A., Cummings R.D.and Baenziger J.U. (2000) Expression cloning of a new member of the ABO blood group glycosyltransferases, iGb3 synthase, that directs the synthesis of isoglobo-glycosphingolipids. *J Biol Chem* **275**, 25308-25314.
35. Ohshima T., Murray G.J., Swaim W.D., Longenecker G., Quirk J.M., Cardarelli C.O.,... and Kulkarni A.B. (1997) alpha-Galactosidase A deficient mice: a model of Fabry disease. *Proc Natl Acad Sci U S A* **94**, 2540-2544.
36. Nguyen Dinh Cat A., Escoubet B., Agrapart V., Griol-Charhbili V., Schoeb T., Feng W.,... and Jaisser F. (2012) Cardiomyopathy and response to enzyme replacement therapy in a male mouse model for Fabry disease. *PloS one* **7**, e33743.
37. Rodrigues L.G., Ferraz M.J., Rodrigues D., Pais-Vieira M., Lima D., Brady R.O.,... and Sa-Miranda M.C. (2009) Neurophysiological, behavioral and morphological abnormalities in the Fabry knockout mice. *Neurobiol Dis* **33**, 48-56.
38. Miller J.J., Aoki K., Mascari C.A., Beltrame A.K., Sokumbi O., North P.E.,... and Dahms N.M. (2019) alpha-Galactosidase A-deficient rats accumulate glycosphingolipids and develop cardiorenal phenotypes of Fabry disease. *FASEB J* **33**, 418-429.
39. Miller J.J., Aoki K., Moehring F., Murphy C.A., O'Hara C.L., Tiemeyer M.,... and Dahms N.M. (2018) Neuropathic pain in a Fabry disease rat model. *JCI Insight* **3**.
40. Mirzaian M., Wisse P., Ferraz M.J., Marques A.R.A., Gaspar P., Oussoren S.V.,... and Aerts J.M. (2017) Simultaneous quantitation of sphingoid bases by UPLC-ESI-MS/MS with identical (13)C-encoded internal standards. *Clin Chim Acta* **466**, 178-184.
41. Driever W.and Rangini Z. (1993) Characterization of a cell line derived from zebrafish (Brachydanio rerio) embryos. *In Vitro Cell Dev Biol Anim* **29A**, 749-754.
42. Rappsilber J., Ishihama Y.and Mann M. (2003) Stop and go extraction tips for matrix-assisted laser desorption/ionization, nanoelectrospray, and LC/MS sample pretreatment in proteomics. *Anal Chem* **75**, 663-670.
43. van Rooden E.J., Florea B.I., Deng H., Baggelaar M.P., van Esbroeck A.C.M., Zhou J.,... and van der Stelt M. (2018) Mapping in vivo target interaction profiles of covalent inhibitors using chemical proteomics with label-free quantification. *Nat Protoc* **13**, 752-767.
44. Groener J.E., Poorthuis B.J., Kuiper S., Helmond M.T., Hollak C.E.and Aerts J.M. (2007) HPLC for simultaneous quantification of total ceramide, glucosylceramide, and ceramide trihexoside concentrations in plasma. *Clin Chem* **53**, 742-747.
45. Tang R., Dodd A., Lai D., McNabb W.C.and Love D.R. (2007) Validation of zebrafish (Danio rerio) reference genes for quantitative real-time RT-PCR normalization. *Acta Biochim Biophys Sin (Shanghai)* **39**, 384-390.